Biochemical Pharmacology, Vol. 39, No. 1, pp. 151–160, 1990.
Printed in Great Britain.

0006-2952/90 $3.00 + .00

A NOVEL MECHANISM OF MYCOPHENOLIC ACID RESISTANCE IN THE PROTOZOAN PARASITE *TRITRICHOMONAS FOETUS*

LIZBETH HEDSTROM, KAM-SING CHEUNG* and CHING C. WANG†
Department of Pharmaceutical Chemistry, School of Pharmacy, University of California, San Francisco, CA 94143, U.S.A.

(*Received* 20 *January* 1989; *accepted* 2 *May* 1989)

Abstract—*Tritrichomonas foetus* relies primarily on the salvage of hypoxanthine to supply purine nucleotides. Mycophenolic acid disrupts *T. foetus* growth by specifically inhibiting inosine-5′-monophosphate (IMP) dehydrogenase, thereby blocking the biosynthesis of guanine nucleotides from hypoxanthine. We have cloned a *T. foetus* strain (mpa^r) that was 50-fold more resistant to mycophenolic acid than wild type (IC_{50} = 1 mM for mpa^r vs 20 μM for wild type). None of the usual mechanisms of drug resistance could be identified. IMP dehydrogenase isolated from *T. foetus* mpa^r was indistinguishable from the wild type enzyme. No difference in mycophenolic acid uptake or metabolism was detected between the wild type and mpa^r strains. Mycophenolic acid (100 μM) completely blocked the conversion of adenine and hypoxanthine to guanine nucleotides in *T. foetus* mpa^r, although no inhibition of *T. foetus* mpa^r growth was observed at this concentration. These observations indicate that the major purine salvage pathways must be altered in *T. foetus* mpa^r so that guanine nucleotide biosynthesis no longer requires IMP dehydrogenase. *T. foetus* mpa^r incorporated xanthine more efficiently into the nucleotide pool relative to hypoxanthine and guanine than wild type. Xanthine incorporation via XMP provided an IMP dehydrogenase independent route to guanine nucleotides that would enable the parasite to become mycophenolic acid resistant. No difference could be detected between wild type and mpa^r hypoxanthine–guanine–xanthine phosphoribosyltransferases, the key enzyme in purine base incorporation into nucleotides. Two alterations were identified in the purine salvage network of mpa^r: it was deficient in hypoxanthine transport and had diminished adenine deaminase activity. The apparent net result of these two changes was to lower the intracellular concentration of hypoxanthine in mpa^r. Hypoxanthine and adenine inhibited the incorporation of xanthine into the nucleotide pool in wild type *T. foetus*, but not in mpa^r. The mpa^r strain, therefore, can salvage xanthine more efficiently from a mixture of purines and thus bypass the drug block at IMP dehydrogenase.

Tritrichomonas foetus is a flagellated anaerobic protozoan parasite that infects the urogenital tract of cattle [1]. Like all protozoan parasites studied to date, *T. foetus* lacks *de novo* purine biosynthesis [2, 3]. This dependence on exogenous purines makes the salvage enzymes attractive targets for chemotherapeutic control of parasitic diseases. The purine salvage pathway of *T. foetus* is shown in Scheme 1 [3]. *T. foetus* prefers to salvage Hyp‡. There is a single phosphoribosyltransferase that is responsible for the conversion of Hyp, Gua and Xan to the corresponding ribose monophosphates [4]. No Ade phosphoribosyltransferase is present. Ade must be deaminated to Hyp prior to incorporation into nucleotides [3]. Inosine-5′-monophosphate (IMP) dehydrogenase is a key enzyme in the biosynthesis of Gua nucleotides from Hyp. We have shown previously that mycophenolic acid (MPA), an inhibitor of IMP dehydrogenase in mammalian cells [5], is an

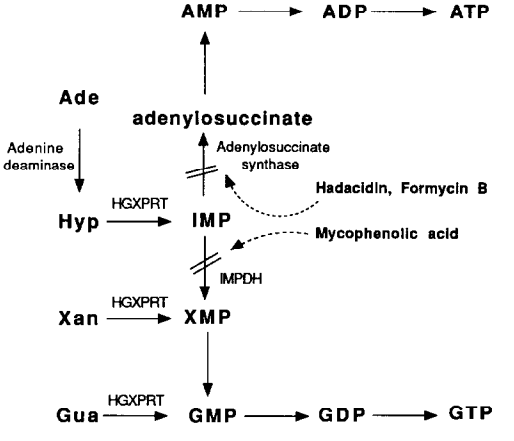

Scheme 1. Purine salvage in *Tritrichomonas foetus*.

* Present address: Block 20, Flat 16D, Chi Fu Fa Yuen, Pokfulam, Hong Kong.

† Burroughs Wellcome Scholar in Molecular Parasitology. Author to whom correspondence should be sent.

‡ Abbreviations: Hyp, hypoxanthine; Ade, adenine; Xan, xanthine; Gua, guanine; IMP, inosine-5′-monophosphate; MPA, mycophenolic acid; mpa^r, mycophenolic acid resistant; NAD, nicotinamide adenine dinucleotide; PRPP, 5′-phosphoribosyl-1-pyrophosphate; TYM, tryptose yeast maltose; DMSO, dimethyl sulfoxide; PBSG, phosphate-buffered saline plus glucose; HGXPRT, hypoxanthine–guanine–xanthine phosphoribosyltransferase; APRT, adenine phosphoribosyltransferase; HPRT, hypoxanthine phosphoribosyltransferase; GPRT, guanine phosphoribosyltransferase; XPRT, xanthine phosphoribosyltransferase; DTT, dithiothreitol; and PIPES, piperazine-*N*,*N*′-bis(2-ethanesulfonic acid).

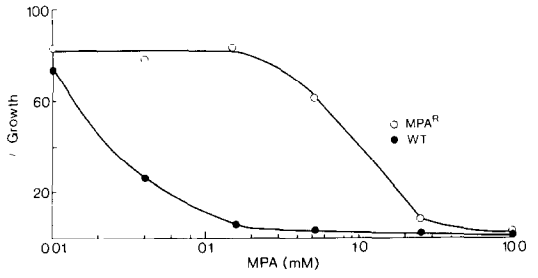

Fig. 1. Effect of MPA on the growth of wild type and mpa^r *T. foetus*. Wild type and mpa^r *T. foetus* were grown in duplicate 1.0-mL cultures of TYM medium containing 0.5% DMSO and the appropriate concentration of MPA. The cultures were started at 1×10^6 cells/mL and grown until the no MPA control reached a density of 1×10^7 (late log phase, 16 hr). Growth is expressed as percentage of the no MPA control. The duplicate samples were within 15% of each other. Cells (100-μL samples) were counted on a Coulter counter ZF. The growth is expressed as percentage of the no drug control.

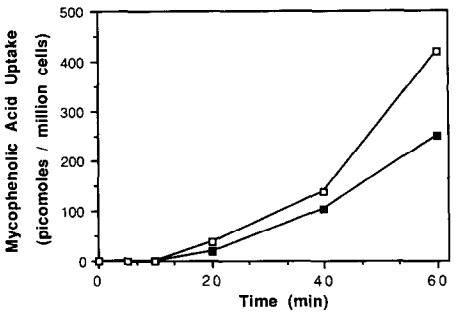

Fig. 2. Uptake of MPA by *T. foetus*. *T. foetus* was harvested in mid-log phase growth ($2–8 \times 10^6$ cells/mL) and resuspended in PBS at 3×10^7 cells/mL. [^{14}C]MPA (200 μM, sp. act. = 4.3×10^9 cpm/mmol) was incubated with *T. foetus* in PBS at 37°. Uptake was measured by centrifuging 100-μL aliquots through dibutyl phthalate, resuspending the pellet in 0.3 M perchlorate, and counting the cell-associated radioactivity as described in Materials and Methods. Key: wild type (■); and mpa^r (□).

inhibitor of *T. foetus* IMP dehydrogenase [6]. MPA also inhibits the growth of *T. foetus in vitro* [7].

Our previous studies indicated that *T. foetus* IMP dehydrogenase is a potential target for chemotherapeutic control [3, 7]. We selected and cloned an MPA resistant strain of *T. foetus* with the expectation of amplifying IMP dehydrogenase or altering the K_i of the enzyme for MPA. Instead we discovered a novel mechanism of drug resistance. The mpa^r strain had decreased its dependence on Hyp salvage. *T. foetus* mpa^r could salvage Xan more efficiently from a mixture of purines and thus bypass the drug block. This is, to our knowledge, the first characterization of an MPA-resistant parasite.

MATERIALS AND METHODS

Materials. [8-^{14}C]Hyp (50 mCi/mmol), [8-^{14}C]Ade (56 mCi/mmol), [8-^{14}C]Xan (56 mCi/mmol) and [8-^{14}C]Gua (56 mCi/mmol) were purchased from ICN Biochemicals. [^{14}C]MPA (42.5 mCi/mmol) was the gift of Dr. Peter Nelson of Syntex. [^{3}H(G)]Ribavirin (10 Ci/mmol) was purchased from Moravek. [^{3}H]H_2O (5 mCi/mmol) and [^{14}C]inulin carboxylic acid (10 mCi/mmol) were obtained from Amersham. IMP, NAD, PRPP and MPA were purchased from Sigma. Ribavirin was the gift of Dr. R. Robbins of the Nucleic Acid Research Institute. TLC plates were obtained from Brinkmann (PEI cellulose) and Kodak (cellulose).

Cell culture. T. foetus strain Kv_1 (wild type) was cultured in Diamonds TYM medium [8] supplemented with 10% heat-inactivated horse serum. The parasites were typically maintained by diluting a stationary culture ($\sim 2 \times 10^7$ cells/mL) 100-fold into 10 mL of fresh medium daily. The mpa^r strain was grown in the presence of 100 μM MPA for at least 1 day prior to each experiment. Wild type *T. foetus* will not grow in 100 μM MPA. Parasites were routinely harvested in mid-logarithmic growth at $2–8 \times 10^6$ cells/mL. Cells were counted by a Coulter Counter ZF.

Analysis of purine metabolism. Purine incorporation into total nucleotides was determined as described previously [3] except that 20-μL aliquots of perchlorate extract were spotted onto PEI cellulose TLC plates in duplicate. The plates were developed twice in 5 mM ammonium acetate, pH 5. The origins were cut out, and the radioactivity was counted in Ecolite (West Chem) in a Beckman LS 3801 liquid scintillation counter. Purine incorporation into individual nucleotides was determined by HPLC analysis on a Beckman Ultrasil-AX anion exchange column with a gradient of 5 mM ammonium phosphate, pH 2.8, to 750 mM ammonium phosphate, pH 3.9, over 50 min at 1 mL/min [9]. The effluent was monitored at 254 nm and mixed 1:3 with Readysolve (Beckman), and radioactivity was measured in a Flo-one radioactivity flow detector (Radiomatic Instruments & Chemical Co.). Purine bases were analyzed by reversed phase HPLC on a C_{18} column (Rainin) with a gradient of 0–25% methanol in 0.1 M potassium phosphate, pH 6.0, over 25 min at 1 mL/min [10]. The purine base content of TYM medium was estimated by HPLC analysis against standard solutions as follows. Hyp and Xan concentrations in TYM medium were determined by measuring A_{254} and monitoring the shift of peaks with Xan oxidase treatment. Gua concentration was estimated from the A_{254} [10]. Ade eluted in a complex region of the TYM chromatogram. Ade concentration in TYM was therefore estimated by adding [^{14}C]Ade to the medium and monitoring the shift of the radioactive peak when treated with excess Xan oxidase. The corresponding decrease in A_{254} was used to estimate the amount of Ade in TYM. The concentrations of purine bases in TYM were as follows: Hyp, 200 μM; Xan, 200 μM; Ade, 40 μM; and Gua $\leq$ 40 μM.

Assay of purine uptake. Purine uptake was measured by a modification of the method of Wohlhueter *et al.* [11]. *T. foetus* cells were washed with PBSG and resuspended at 7×10^8 cells/mL. The cell suspension (200 μL) was added to 200 μL of [^{14}C]purine (500 cpm/μL) in PBSG layered over 300 μL of dibutyl phthalate in 1.5-mL Eppendorf

tube at 23°. The tubes were centrifuged for 15 sec, the aqueous layer was removed, and the oil was overlayered with 1 mL of H_2O as a wash. The liquid layers were removed, the cell pellet was resuspended in 125 μL of 0.3 M perchlorate, and the radioactivity was counted. Similar experiments using [^{3}H]H_2O as the permeant to determine total pellet volume and [^{14}C]inulin to determine extracellular volume were also performed as controls. Typically the pellet of 1.4×10^8 cells had a total volume of 22 μL and an extracellular volume of 2 μL.

A time course for the intracellular concentration of Ade and Hyp was determined in a similar experiment except that the cell suspension was layered over a 600 μL dibutyl phthalate which was layered over 300 μL of 0.3 M perchloric acid in 15% sucrose. The aqueous and oil layers were removed as before, and the sucrose layer was adjusted to pH 7 with KOH and analyzed by HPLC as described above. The deamination of Ade to Hyp was confirmed by treatment with Xan oxidase.

Enzyme assays. Crude extracts were prepared from cells in mid-logarithmic growth. The cells were washed three times with 50 mM Tris, pH 7.4, 1 mM DTT and resuspended in 4 vol. of 50 mM Tris, pH 7.4, 1 mM DTT, 5 mM $MgCl_2$, 1 mM PRPP (for phosphoribosyltransferase assays) or 20 mM KCl (for Ade deaminase assays). To prepare crude extracts, the cells were sonicated, and then centrifuged to remove cell debris. Extracts assayed for Ade deaminase were desalted with a Sephadex G50 spin column (Boehringer Mannheim). IMP dehydrogenase was partially purified as described previously [6]. HGXPRT was partially purified for K_m determinations by Sephadex G100 chromatography. Crude extract (1–5 mL) was applied to a 100-mL column equilibrated with 1 mM PRPP, 5 mM $MgCl_2$, 50 mM Tris–Cl, pH 7.4, 1 mM DTT. The HGXPRT activity was purified approximately 20- to 30-fold to a specific activity of 71 nmol IMP produced/min/mg (wild type) and 32 nmol IMP produced/min/mg (mpa^r). Protein concentration was determined by the method of Bradford [12] with bovine IgG as a standard. All spectrophotometric measurements were made on a Beckman DU-7 UV-visible spectrophotometer.

IMP dehydrogenase was assayed spectrophotometrically at 37° [13]. The assay mix contained 50 mM Tris, pH 8.1, 100 mM KCl, 2 mM DTT, 0.2 mM IMP and 0.26 mM NAD. Phosphoribosyltransferase activity was assayed in 0.1 mM [^{14}C]purine, 1 mM PRPP, 5 mM $MgCl_2$ and 50 mM Tris, pH 7.8, at 37°. Enzyme was added to start the reaction and aliquots (10 μL) were spotted onto cellulose TLC plates pre-spotted with the base, nucleoside and nucleotide monophosphate. The chromatogram was developed in H_2O. Ade deaminase was assayed in 0.2 mM [^{14}C]Ade, 1 mM $MgCl_2$, 50 mM KCl and 20 mM PIPES, pH 6.8. Enzyme was added to start the reaction and 100-μL aliquots were quenched with 5 μL of 4.2 M perchloric acid. The protein was removed by centrifugation, and the supernatant fraction was adjusted to pH 7 with KOH. The samples were analyzed by HPLC on a C_{18} column [10].

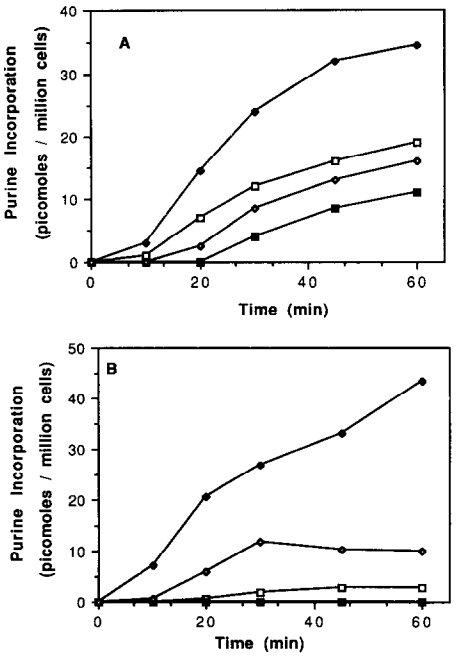

Fig. 3. Purine base incorporation into nucleotides in *T. foetus*. *T. Foetus* was harvested in log phase growth (2–8 × 10^6 cells/mL) and resuspended in PBSG at 7 × 10^7 cells/mL. The parasites were incubated with [^{14}C]purines (20 μM, 50 mCi/mmol) in PBSG at 37°. Aliquots (100 μL) were quenched with 5 μL of 4.2 M perchloric acid. The cell debris was removed by centrifugation and the solution was neutralized with KOH to remove the perchlorate. Nucleotide incorporation was determined by the binding of radioactivity to PEI cellulose as described in Materials and Methods. Key: (A) wild type; (B) mpa^r; Ade (◆); Hyp (□); Xan (◇; and Gua (■).

RESULTS

Cloning of the MPA-resistant strain of T. foetus. MPA is toxic to *T. foetus* Kv_1 with an IC_{50} of 20 μM [7] when cultured on TYM medium. TYM medium is a complex undefined medium which contains 200 μM Hyp, 200 μM Xan, 40 μM Ade and less than 40 μM Gua. An MPA-resistant strain of *T. foetus* was obtained by culturing the parasite in stepwise increasing concentrations of MPA, from 16 μM to 2 mM in 9 steps over 7 weeks. The resistant population was cloned by cultivation on agar plates [9]. One colony, *T. foetus* mpa^r, was chosen for further study. This strain was 50-fold more resistant to MPA than the wild type with an IC_{50} of 1 mM MPA, as shown in Fig. 1. The mpa^r had a doubling time of 4 hr in TYM medium in the presence of 100 μM MPA, which is identical to the doubling time of wild type *T. foetus* in TYM in the absence of drug. The strain can be cultured in the absence of MPA for months without loss of MPA resistance.

IMP dehydrogenase activity in T. foetus *mpa^r*. Drug resistance often results from a change in the target enzyme of the drug. MPA is a specific inhibitor of IMP dehydrogenase from mammalian sources [5, 14] as well as *T. foetus* [6, 7]. A change in IMPDH in *T. foetus* mpa^r could account for MPA resistance. No significant difference could be detected in the

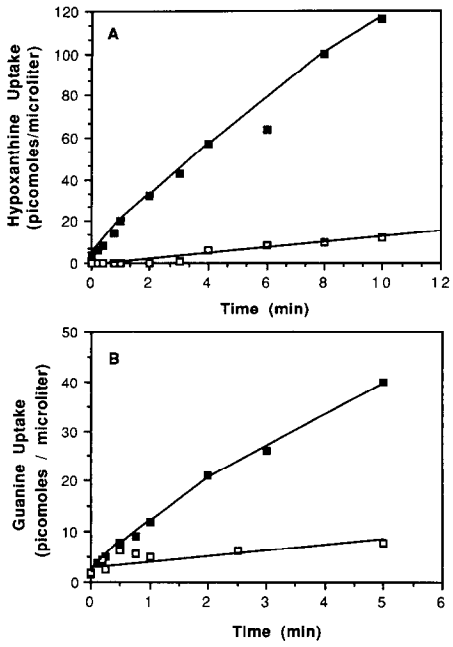

Fig. 4. Hyp and Gua uptake in *T. foetus*. (A) Uptake of Hyp. *T. foetus* was harvested in mid-log phase growth (2–8 × 10^6 cells/mL) and resuspended in PBSG at 7 × 10^8 cells/mL. The parasites (200 μL) were pipetted vigorously into 200 μL of [^{14}C]Hyp (200 μM) in PBSG at 23° layered over 300 μL of dibutyl phthalate in a 1.5-mL Eppendorf microfuge tube. The final concentration of Hyp was 100 μM (550 cpm/μL) and of parasites was 3.5 × 10^8 cells/mL. Transport was quenched by centrifugation. The zero time point is uncorrected for the time between addition of parasites and centrifugation (approximately 1–2 sec). The volume of the cell pellet was determined by incubating in [^{3}H]H_2O (820 cpm/μL), which measures the total pellet volume (wild type: 22.4 ± 0.5 μL; mpa^r: 12.9 ± 0.3 μL) and [^{14}C]inulin, which measures the extracellular space (wild type: 2.4 ± 0.2 μL; mpa^r: 1.6 ± 0.3 μL). The data are corrected for the amount of [^{14}C]Hyp in the extracellular space. Keys: wild type (■); and mpa^r (□); (B) Uptake of Gua. As above, but the final concentration of Gua was 50 μM (660 cpm/μL). Total cell volume; wild type, 22.6 ± 0.3 μL; mpa^r; 11.3 ± 0.2 μL. Extracellular volume; wild type, 2.6 ± 0.3 μL; mpa^r; 1.5 ± 0.2 μL. Key: wild type (■); and mpa^r (□).

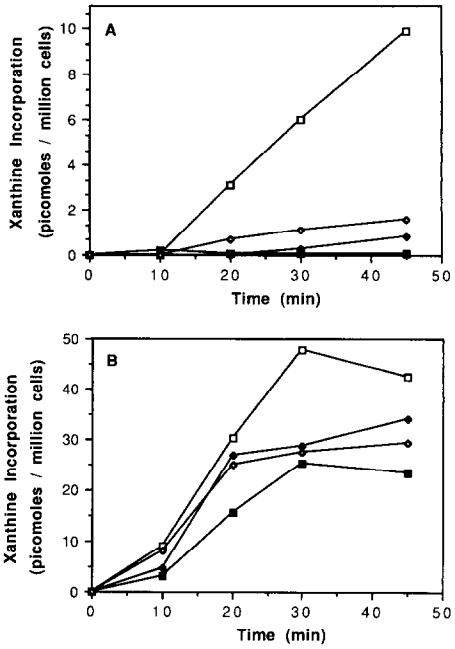

Fig. 5. Inhibition of Xan incorporation into nucleotides by *T. foetus*. *T. foetus* (7 × 10^7 cells/mL) was incubated with [^{14}C]Xan (20 μM) in PBSG at 37° in the presence of the following additions: none (□); Hyp (◆); Gua (◇); and Ade (■) (200 μM). Incorporation of Xan into nucleotides was measured as described in the legend of Fig. 3. Key: (A) wild type, and (B) mpa^r.

IMP dehydrogenase levels in crude extracts from wild type (sp. act. = 1.0 nmol/min/mg) or mpa^r *T. foetus* (sp. act. = 1.4 nmol/min/mg). IMP dehydrogenase from mpa^r was partially purified to sp. act. = 670 nmol/min/mg. This enzyme had kinetic parameters very similar to those previously reported for the wild type enzyme [6]: K_m(IMP) = 7 μM for *T. foetus* mpa^r vs 20 μM for wild type; K_m (NAD) = 270 μM vs 340 μM and K_i (MPA) = 6 μM vs 9 μM. Thus, no difference that could account for the 50-fold resistance to MPA could be detected between IMP dehydrogenases from wild type and mpa^r strains.

MPA metabolism. Drug resistance can also result from a decrease in drug uptake or by conversion of the drug to an inactive metabolite. The rates of MPA uptake were similar for wild type and mpa^r *T. foetus*. A typical experiment is shown in Fig. 2. No conversion of MPA to other compounds could be detected in either strain by TLC analysis. Thus, no difference in drug uptake or metabolism was detected that could account for MPA resistance. To substantiate that MPA was indeed blocking IMPDH in *T. foetus* mpa^r, the incorporation of Hyp and Ade into nucleotides was monitored as shown in Table 1. Hyp and Ade incorporation into Gua nucleotides was inhibited in both mpa^r and wild type in the presence of 100 μM MPA. [^{14}C]Hyp was not converted to Gua di- and triphosphates in the presence of 100 μM MPA in mpa^r, though this concentration of MPA had no effect on *T. foetus* mpa^r growth. Similar results were obtained with [^{14}C]Ade. These results indicate that MPA blocks IMPDH in the resistant parasite. Therefore, purine salvage must be altered in *T. foetus* mpa^r so that Gua nucleotide biosynthesis no longer requires IMP dehydrogenase.

Purine incorporation into nucleotides in T. foetus *mpa^r*. An increase in Xan or Gua salvage could provide an IMP dehydrogenase independent route to Gua nucleotides (see Scheme 1). The incorporation of individual [^{14}C]purine bases (20 μM) into the total nucleotide pool was monitored to test this hypothesis. A typical experiment is shown in Fig. 3. Wild type incorporated Ade most efficiently under these conditions, followed by Hyp, Xan, and Gua. Mpa^r also incorporated Ade most efficiently, but Xan was consistently incorporated at much higher levels than Hyp and Gua. The actual amount (pmol/10^6 cells) of purine base incorporated into nucleotides varied with each batch of cultured parasites.

Table 1. Effects of purine antimetabolites on the incorporation of hypoxanthine and adenine into the purine nucleotide pool of *T. foetus*

Experiment	Strain	% Incorporation			
		ADP	ATP	GDP	GTP
[^{14}C]Hyp + 100 μM MPA	Wild type (2)*	210 ± 30	190 ± 10	2 ± 2	4 ± 4
	mpa^r (2)†	200 ± 100	110 ± 10	8 ± 8	3 ± 3
[^{14}C]Ade + 100 μM MPA	Wild type (2)‡	260 ± 20	270 ± 30	12 ± 1	8 ± 5
	mpa^r (2)§	200 ± 40	200 ± 40	3 ± 3	4 ± 4
[^{14}C]Ade + 5 mM Hadacidin	Wild type (2)‖	10 ± 10	10 ± 8	110 ± 10	120 ± 20
	mpa^r (2)¶	25 ± 5	23 ± 7	110 ± 20	140 ± 30
[^{14}C]Ade + 1 mM FoB	Wild type (3)**	16 ± 8	8 ± 8	100 ± 30	200 ± 100
	mpa^r (2)††	13 ± 5	14 ± 1	110 ± 30	88 ± 1

T. foetus (7×10^7 cells/mL) was incubated with 20 μM [^{14}C]Hyp (50 mCi/mmol) or [^{14}C]Ade (56 mCi/mmol) at 37° for 45 min in PBSG in the presence or absence of mycophenolic acid (MPA), formycin B (FoB) (1 mM) and hadacidin (5 mM). The nucleotide pools were extracted with perchlorate and analyzed by HPLC as described in Materials and Methods. Radioactivity was measured with a radioactivity flow detector (Radiomatic Instruments). The data are expressed as the percent of the radioactivity incorporated into the particular nucleotide in the no drug control. The number in parentheses after the strain is the number of determinations. Values are means ± SD.

The radioactivity flow detector reports in "cpm". The noise level is 6 cpm.

* 100% values were: ADP, 254 and 434 cpm; ATP, 1044 and 1244 cpm; GDP, 245 and 249 cpm; GTP, 902 and 746 cpm.

† 100% values were: ADP, 33 and 160 cpm; ATP, 322 and 318 cpm; GDP, 82 and 29 cpm; GTP, 173 and 84 cpm.

‡ 100% values were: ADP, 768 and 357 cpm; ATP, 2081 and 761 cpm; GDP, 832 and 382 cpm; GTP, 1847 and 727 cpm.

§ 100% values were: ADP, 512 and 362 cpm; ATP, 1067 and 641 cpm; GDP, 199 and 417 cpm; GTP, 548 and 1026 cpm.

‖ 100% values were: ADP, 234 and 357 cpm; ATP, 584 and 761 cpm; GDP, 179 and 382 cpm; GTP, 607 and 727 cpm.

¶ 100% values were: ADP, 400 and 362 cpm; ATP, 1099 and 641 cpm; GDP, 80 and 417 cpm; GTP, 286 and 1026 cpm.

** 100% values were: ADP, 207 and 357 cpm; ATP, 74 and 761 cpm; GDP, 336 and 382 cpm; GTP, 62 and 727 cpm.

†† 100% values were: ADP, 800 and 362 cpm; ATP, 1107 and 641 cpm; GDP, 782 and 417 cpm; GTP, 1146 and 1026 cpm.

Therefore it is not valid to compare the amount of purine base incorporation between strains. However, the order of preference was always maintained. Hyp incorporation into nucleotides was favored 2-fold over Xan in wild type in the linear region of incorporation, while Xan was favored 6-fold over Hyp in mpa^r. This relationship was observed in at least three independent experiments. Therefore, it appears that *T. foetus* mpa^r is resistant to MPA by increasing the incorporation of Xan into nucleotides relative to Hyp, thus decreasing the dependence of the resistant parasite on Hyp (and IMPDH) for the biosynthesis of Gua nucleotides (Scheme 1).

HGXPRT activity in T. foetus *mpa^r*. Phosphoribosylation is the key step in the incorporation of a purine base into the nucleotide pool. *T. foetus* has a single phosphoribosyltransferase that catalyzes the conversion of Hyp, Gua and Xan into the corresponding nucleoside monophosphates [4]. It seemed likely that a mutation in this enzyme could be responsible for the increase in Xan over Hyp incorporation into nucleotides. HGXPRT activities were assayed in wild type and mpa^r crude extracts, as shown in Table 2. The phosphoribosyltransferase activities in crude extracts from the two strains were nearly identical for all three purine bases. No significant differences were detected in the K_m, values for Hyp, Gua, Xan or PRPP between enzyme from the two sources. Further, Gua and Hyp competitively inhibited Xan phosphoribosylation identically for enzymes from both sources (data not shown). Therefore, the increase in Xan incorporation into nucleotides over Hyp cannot be attributed to a change in HGXPRT in the mpa^r strain.

Hyp transport in T. foetus. The incorporation of a purine base into the nucleotide pool requires its transport into the cell and its subsequent phosphoribosylation. The failure to observe a change in HGXPRT in the mpa^r strain suggested that purine transport might be altered. A change in purine transport could cause the differences in purine incorporation into nucleotides observed in mpa^r *T. foetus* (Fig. 3). We will use "uptake" to denote the net accumulation of a purine in a cell, regardless of its subsequent metabolism, and "transport" to denote the translocation of a purine into a cell. Parasites were incubated with 100 μM [^{14}C]Hyp. Uptake was stopped by centrifugation through dibutyl phthalate, as described in Materials and Methods. Figure 4A shows that Hyp uptake was reduced in mpa^r relative to wild type *T. foetus*. Several observations suggest that this experiment measured transport, not Hyp incorporation into nucleotides. Incorporation into nucleotides affects uptake by trapping Hyp within the cell. When the intracellular concentration is

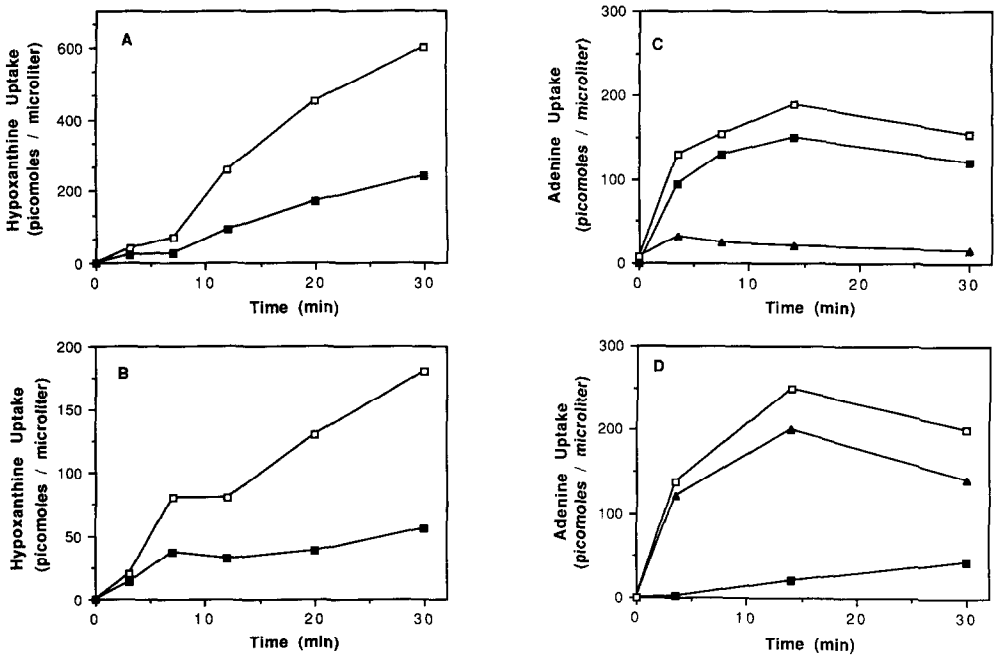

Fig. 6. Intracellular Hyp and Ade concentration in *T. foetus*. (A) Wild type *T. foetus* and intracellular Hyp. [^{14}C]Hyp (200 μM, 4000 cpm/μL) was incubated with parasites in PBSG at 37° as described in the legend of Fig. 4 except that an additional layer of 300 μL of 0.3 M perchlorate in 15% sucrose was under the dibutyl phthalate layer. The perchlorate layer quenched metabolism and extracts were prepared as in Fig. 3. The samples were analyzed for [^{14}C]Hyp by reversed phase HPLC with a radioactivity flow detector as described in Materials and Methods. The volumes of the cell pellet (35 ± 1 μL) and extracellular space (8.1 ± 0.5 μL) were determined with [^{3}H]H_2O and [^{14}C]inulin. The intracellular concentration of total radioactivity (□) is shown as well as the intracellular concentration of Hyp (■). (B) Mpa^r *T. foetus* and intracellular Hyp. As described above. Total cell volume: 45 ± 2 μL; extracellular volume: 11.4 ± 0.3 μL. Key: total radioactivity (□) and Hyp (■). (C) Wild type *T. foetus* and intracellular Ade. [^{14}C]Ade (200 μM, 3300 cpm/μL) was incubated with parasites in PBSG at 37°. Metabolism was measured by an oil stop method with a perchloric acid quench as described above. Ade and Hyp were analyzed by reversed phase HPLC. Total cell volume: 22.1 ± 0.1 μL; extracellular volume: 0.6 ± 0.1 μL. Key: total radioactivity (□); Ade (▲); and Hyp (■). (D) Mpa^r *T. foetus* and intracellular Ade. As described above. Total cell volume: 24.9 ± 0.2 μL; extracellular volume: 0.6 ± 0.1 μL. Key: total radioactivity (□); Ade (▲); and Hyp (■).

much less than the extracellular concentration of Hyp, the rate of uptake is limited by the rate of transport. Incorporation into nucleotides will have no effect on the rate of uptake under these conditions because Hyp is already trapped in the cell by the high extracellular concentration of Hyp. When the intracellular concentration of Hyp is equal to the extracellular concentration, the rate of uptake is determined by the rate of incorporation into nucleotides. If Hyp transport is identical in the two strains, the rate of uptake of Hyp should be identical when the intracellular concentration of Hyp is much less than the extracellular concentration, i.e. under conditions where transport limits uptake. A difference in metabolism will only be observed when the intracellular Hyp approximates the extracellular concentration. Figure 4A shows that wild type *T. foetus* accumulated [^{14}C]Hyp at 20 pmol/μL/min when the total amount of Hyp and its nucleotides was less than 25 μM and the extracellular Hyp was 100 μM. In contrast, the rate of [^{14}C]Hyp uptake in mpa^r was 1.3 pmol/μL/min, which was 7% the rate of wild type. It is important to note that the uptake of Hyp by mpa^r remained much less than the extracellular concentration for at least 30 min. This can only be explained by a defect in transport. Wild type reached extracellular concentrations in approximately 8 min. Hyp uptake was ~10-fold faster in wild type than mpa^r at all concentrations of Hyp tested (0.01 to 1.0 mM) (data not shown). The rate of uptake was constant from one batch of parasites to another (within 50% for at least five independent experiments).

Similar results were obtained with Gua uptake. Figure 4B shows that Gua uptake was also much slower in mpa^r than in wild type *T. foetus*. Again, mpa^r did not accumulate Gua to extracellular concentrations in 5 min, although wild type Gua uptake did reach extracellular levels. This suggests that transport, not metabolism was measured. No difference was observed in Ade or Xan transport (data not shown) between wild type and mpa^r. The decrease in Hyp and Gua transport can explain the decrease in Hyp and Gua incorporation into the mpa^r nucleotide pool observed in Fig. 3.

Inhibition of Xan incorporation into nucleotides. The decrease in Hyp and Gua transport does not explain MPA resistance in *T. foetus* mpa^r. However,

Table 2. Hypoxanthine–guanine–xanthine phosphoribosyltransferase activity in *T. foetus*

Sample	Specific activity (nmol/min/mg)	HPRT activity K_m (H) (μM)	K_m (PRPP) (μM)
Wild type	2.5 ± 0.6 (4)	4.9 ± 0.8 (3)	60 ± 20 (2)
mpa^r	3.9 ± 0.8 (4)	4.5 ± 0.5 (2)	50 ± 20 (3)
Sample	Specific activity (nmol/min/mg)	GPRT activity K_m (G) (μM)	K_m (PRPP) (μM)
Wild type	1.7 ± 0.4 (3)	4 ± 1 (4)	30 ± 4 (2)
mpa^r	1.5 ± 0.6 (4)	4 ± 2 (3)	17 ± 3 (2)
Sample	Specific activity (nmol/min/mg)	XPRT activity K_m (X) (μM)	K_m (PRPP) (μM)
Wild type	2.4 ± 0.4 (3)	58 ± 5 (2)	30 ± 10 (2)
mpa^r	2.5 ± 0.5 (3)	70 ± 20 (3)	20 ± 10 (2)

Crude extracts were prepared from wild type and mpa^r *T. foetus*, as described in Materials and Methods. The specific activities in crude extracts were determined at 100 μM purine base, 1.0 mM PRPP, 5.0 mM $MgCl_2$ in Tris, pH 7.8. The enzyme was partially purified on a Sephadex G100 column for K_m determinations (sp. act. = 70 nmol/min/mg HPRT for wild type and 30 nmol/min/mg HPRT for mpa^r). Abbreviations: HPRT, hypoxanthine phosphoribosyltransferase; GPRT, guanine phosphoribosyltransferase; XPRT, xanthine phosphoribosyltransferase; H, hypoxanthine; G, guanine; X, xanthine. K_m values for purine bases were determined in the presence of 1.0 mM PRPP, while the K_m values for PRPP were determined in the presence of 100 μM purine base. Values are means ± SD. The numbers in parentheses are the number of independent experiments.

the increase in Xan incorporation into the nucleotide pool can explain MPA resistance (Fig. 3). We therefore postulated that the intracellular accumulation of Hyp inhibits Xan incorporation into nucleotides. Such inhibition is a common feature of many biological systems. A decrease in Hyp transport would relieve this inhibition and allow Xan to be salvaged more efficiently from a mixture of purines. Figure 5 suggests that this is indeed the case. [^{14}C]Xan (20 μM) incorporation into the nucleotide pool was strongly inhibited by the presence of 200 μM Hyp, Gua and Ade in wild type *T. foetus*. No inhibition of [^{14}C]Xan incorporation into the nucleotide pool was observed by 200 μM inosine, adenosine, guanosine or xanthosine in a similar experiment. In contrast, little inhibition of [^{14}C]Xan incorporation into nucleotides by Hyp, Gua and Ade was observed in mpa^r (Fig. 5). Wild type and mpa^r XPRT activities were inhibited similarly by Hyp and Gua. Therefore, the loss of Hyp and Gua inhibition of Xan incorporation into nucleotides in mpa^r cannot be attributed to a change in the HGXPRT. The failure of Hyp and Gua to inhibit Xan incorporation into nucleotides in mpa^r can be attributed to the decreased transport of these two purines. However, the failure of Ade to inhibit Xan incorporation into nucleotides in mpa^r observed in Fig. 5 was unexpected. Ade did not inhibit the HGXPRT (data not shown). In wild type *T. foetus* Ade is not salvaged directly, but must first be converted to Hyp (Scheme 1) [3]. Ade uptake was similar for both wild type and mpa^r. Therefore, Ade would be expected to inhibit Xan incorporation in mpa^r. This suggests that Ade metabolism is also altered in mpa^r.

Ade metabolism in T. foetus *mpa^r*. Ade incorporation into nucleotides requires transport into the parasite, deamination to Hyp, and phosphoribosylation by HGXPRT (Scheme 1). Ade transport and HGXPRT activity were identical in the two strains (see above), which suggests that Ade deaminase had been altered. A decrease in Ade deaminase in the mpa^r strain was confirmed by assays of crude extracts in both mid and late log phase parasites. The enzyme activity did not change in the two phases of growth. Wild type crude extract had a specific activity of 1.1 ± 0.5 nmol/min/mg protein, which was 50-fold higher than the mpa^r Ade deaminase activity of 0.02 ± 0.01 nmol/min/mg protein (average of three experiments).

Ade was incorporated into nucleotides efficiently in *T. foetus* mpa^r as judged by Fig. 3 despite the decrease in Ade deaminase activity. Ade is converted to Hyp prior to incorporation into nucleotides in wild type *T. foetus* [3]. No APRT activity could be detected in crude extracts of mpa^r *T. foetus*, which suggests that Ade cannot be incorporated directly into nucleotides in mpa^r *T. foetus*. An experiment was designed to confirm the absence of APRT activity in whole parasites. The incorporation of [^{14}C]Ade into the nucleotide pool was monitored in the presence and absence of the adenylosuccinate synthase inhibitors hadacidin [15] and formycin B [16]. Hadacidin did not inhibit the growth of either wild type or mpa^r at 10 mM, whereas formycin B was toxic to both wild type and mpa^r *T. foetus* with IC_{50} = 30 μM (data not shown). Our previous studies indicated that both hadacidin and formycin B inhibit the incorporation of [^{14}C]Hyp into Ade nucleotides

in wild type *T. foetus*, indicating that these compounds inhibit *T. foetus* adenylosuccinate synthase [7]. If Ade is incorporated into nucleotides by an APRT, hadacidin and formycin B should have no effect on the conversion of [^{14}C]Ade to Ade nucleotides. Table 1 shows that hadacidin (5 mM) and formycin B (1 mM) inhibited the incorporation of [^{14}C]Ade into Ade nucleotides. Hadacidin and formycin B had little effect on the incorporation of [^{14}C]Ade into Gua nucleotides. These data suggest that there is no APRT activity in either wild type or mpa^r *T. foetus* and that Ade is usually converted to Hyp prior to incorporation into the nucleotide pool (see Discussion).

Intracellular Hyp concentrations in wild type and mpa^r T. foetus. The above experiments suggest that the intracellular concentration of Hyp is high in wild type *T. foetus* relative to mpa^r when incubated with either Hyp or Ade. We measured the intracellular Hyp concentrations directly as shown in Fig. 6. Figure 6A shows that, when wild type *T. foetus* was incubated with 200 μM [^{14}C]Hyp, intracellular Hyp accumulated to concentrations equal to the extracellular Hyp concentration. In contrast, the intracellular concentration of Hyp reached steady state of 40 μM for *T. foetus* mpa^r, which was one-fifth the extracellular Hyp concentration. In a second experiment, wild type again accumulated intracellular [Hyp] to 200 μM, while mpa^r intracellular [Hyp] reached steady state at 20 μM. Therefore, the mpa^r strain does indeed have much lower intracellular [Hyp] than wild type.

The decrease in Ade deaminase activity observed in *T. foetus* mpa^r suggested that the intracellular concentration of Hyp resulting from the deamination of Ade would be lower in mpa^r than in wild type. Panels C and D of Fig. 6 show that this was observed. When parasites were incubated with [^{14}C]Ade, total radioactivity accumulated at similar rates for wild type and mpa^r. These data agree with our previous observation that the rate of Ade transport was the same for both strains [17]. Wild type *T. foetus* deaminated Ade to Hyp very rapidly, as shown in Fig. 6C. The steady-state concentration of Hyp was very high in these cells (150 μM) which accounts for the Ade inhibition of Xan incorporation into nucleotides in wild type (Fig. 5). In contrast, mpa^r had very low Hyp concentrations (<40 μM), and the rate of Ade conversion to Hyp appeared much slower (Fig. 6D). Therefore, there was little inhibition of Xan incorporation into nucleotides in mpa^r. Hyp and Ade contained 90% of the recovered radioactivity in both wild type and mpa^r.

Model for MPA resistance. T. foetus mpa^r apparently has two alterations in its purine metabolism: it is deficient in Hyp and Gua transport and Ade deaminase activity. The net result of these mutations is to lower the intracellular concentration of Hyp. This enables Xan to be incorporated into the nucleotide pool more efficiently by relieving the Hyp inhibition. Three experiments were performed to test this model. First, *T. foetus* mpa^r should be resistant to other IMP dehydrogenase inhibitors in addition to MPA. Ribavirin is a nucleoside analog that inhibits IMP dehydrogenase in its monophosphate form [18]. Ribavirin monophosphate was a potent inhibitor of

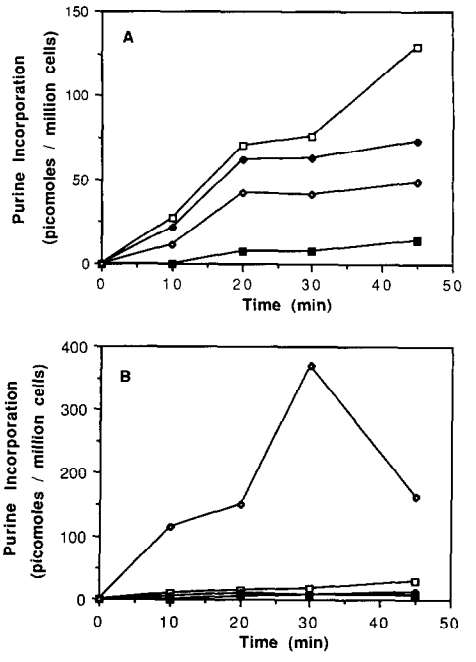

Fig. 7. Purine salvage in TYM medium by *T. foetus*. [^{14}C]Purines were added to TYM as follows: 3000 cpm/μL [^{14}C]Hyp (◆), 3500 cpm/μL [^{14}C]Ade (□), 2200 cpm/μL [^{14}C]Gua (■) or 2200 cpm/μL [^{14}C]-Xan (◇). the concentrations of purine bases in TYM were: Hyp, 200 μM; Ade, 40 μM; Xan, 200 μM; Gua ≤ 40 μM. Incorporation of purines into nucleotides was measured as described in the legend of Fig. 3. Keys: (A) wild type, and (B) mpa^r.

T. foetus IMP dehydrogenase [17]. Ribavirin inhibited the growth of wild type *T. foetus* with an IC_{50} of 30 μM. *T. foetus* mpa^r was resistant to ribavirin: no inhibition of growth was observed in 1 mM ribavirin. Ribavirin uptake and metabolism to mono-, di- and triphosphates were identical in both strains (data not shown). Therefore, it is likely that the resistance of the mpa^r strain to ribavirin results from the same mechanism that provides MPA resistance.

Second, TYM medium, which was used to select the mpa^r mutant, is a complex mixture of purine bases and nucleosides. The model predicts that Xan incorporation into nucleotides in TYM medium should be increased relative to Hyp, Ade and Gua for mpa^r when compared with wild type. Purine base incorporation into nucleotides in TYM was measured by adding [^{14}C]purines to the medium. A typical experiment is shown in Fig. 7. Wild type *T. foetus* incorporated Hyp and Ade into the nucleotide pool most efficiently from TYM, whereas Xan was incorporated at about half the rate of Ade and Hyp. Gua was not incorporated into the nucleotide pool very efficiently from TYM medium in wild type *T. foetus*. This suggests that wild type *T. foetus* relies primarily on the salvage of Hyp and Ade to provide purine nucleotides when growing on TYM medium. In contrast, mpa^r salvaged Xan preferentially from TYM, incorporating Xan into the nucleotide pool at least ten times faster than Hyp, Ade or Gua (Fig. 7). Thus, mpa^r had switched from Hyp and Ade salvage to Xan salvage to provide purine nucleotides when grown on TYM medium.

DISCUSSION

We have discovered a novel mechanism of drug resistance in the protozoan parasite *T. foetus*. MPA is a specific inhibitor of IMP dehydrogenase and therefore blocks the conversion of Hyp to Gua nucleotides. MPA is toxic to *T. foetus* [7] as well as many mammalian tumor lines [5, 19]. Several mechanisms of MPA resistance have been observed in mammalian cells: (1) increased levels of the target enzyme IMP dehydrogenase [20]; (2) change in the substrate binding of IMP dehydrogenase [21]; (3) conversion of MPA to an inactive metabolite [22]; (4) increased Hyp–Gua phosphoribosyltransferase activity [22]; and (5) the acquistion of Xan phosphoribosyltransferase activity [23]. Decrease in MPA uptake is also a likely mechanism, although it has not yet been observed. We have cloned an MPA-resistant strain of *T. foetus*. Resistance did not result from any of the above mechanisms. Instead, *T. foetus* mpa^r rearranged its salvage pathways to reduce its dependence on Hyp and incorporate Xan into the nucleotide pool more efficiently. The utilization of Xan as the primary source of purine nucleotides allowed *T. foetus* mpa^r to bypass the MPA-sensitive step, IMP dehydrogenase (Scheme 1).

Two key observations support this mechanism. First, Xan was incorporated into nucleotides more efficiently than Hyp in *T. foetus* mpa^r, as shown in Figs. 3 and 7. Second, Xan incorporation into nucleotides was no longer inhibited by Hyp, Gua or Ade in *T. foetus* mpa^r as shown in Fig. 5. The relief of this inhibition allowed *T. foetus* mpa^r to preferentially incorporate Xan into the nucleotide pool from a mixture of purines such as TYM medium (Fig. 7). Two defects were identified: mpa^r was deficient in Hyp and Gua transport and in Ade deaminase activity. The net effect of these two alterations was to lower the intracellular concentration of Hyp and relieve Hyp inhibition of Xan incorporation into the nucleotide pool. Wild type accumulated intracellular Hyp to concentrations equal to extracellular Hyp, whereas mpa^r intracellular Hyp reached steady state at concentrations much lower than extracellular Hyp (Fig. 6). This indicates that Hyp transport is much faster than phosphoribosylation in wild type, while Hyp transport is reduced in mpa^r so that the rate of transport is similar to the rate of phosphoribosylation.

The decrease in Hyp transport may result from the loss of a specific carrier. The accompanying decrease in Gua transport suggests that the mutant may have lost a single carrier that is responsible for both Hyp and Gua transport. Hyp–Gua transporters have been identified in many systems [24, 25]. We are presently characterizing the purine transport system in wild type and mpa^r *T. foetus*. The loss of Gua transport and the decrease in Gua incorporation into nucleotides seem counterproductive for an organism struggling to make Gua nucleotides. Figure 7 suggests that Gua incorporation into the nucleotide pool is not very important for purine metabolism in wild type *T. foetus* cultured on TYM medium, possibly because TYM medium contains less than 40 μM Gua. There may not be sufficient Gua concentrations in TYM to provide MPA resistance.

In addition to the defect in Hyp and Gua transport, mpa^r has diminished Ade deaminase activity. The decrease in Ade deaminase activity may result from a reduction in enzyme levels or a change in the enzyme itself. The production of a specific inhibitor of Ade deaminase in the mpa^r strain is unlikely because crude extracts from mpa^r did not inhibit Ade deaminase activity in wild type crude extracts (data not shown). The nature of the defect at the molecular level is not known.

The decrease in Ade deaminase activity in mpa^r apparently contradicts the observation that Ade was efficiently incorporated into the nucleotide pool in mpa^r *T. foetus* (Fig. 3). It is unlikely that Ade was incorporated into nucleotides by an alternative pathway that did not involve Hyp. The incorporation of [^{14}C]Ade into Ade nucleotides was inhibited by two different adenylosuccinate synthase inhibitors: hadacidin (an aspartate analog) [15] and formycin B (an inosine analog) [16] (Table 1), which indicates that adenylosuccinate synthase is an obligatory step in Ade nucleotide biosynthesis. This eliminates the possibility that Ade is incorporated into nucleotides via an APRT or adenosine phosphorylase and adenosine kinase [3].* A third possibility is that Ade is incorporated via adenosine → inosine → IMP, which would require adenylosuccinate synthase for the biosynthesis of Ade nucleotides. This pathway might explain the efficient incorporation of Ade into the nucleotide pool by mpa^r despite the decrease in Ade deaminase activity. A more likely explanation is that Ade deaminase was not the rate-limiting step for Ade incorporation into nucleotides under the conditions of Fig. 3. Therefore, a decrease in Ade deaminase activity would not affect Ade incorporation into nucleotides. Figure 7 does show that Ade incorporation into the mpa^r nucleotide pool from TYM medium was decreased, probably due to the defect in Ade deaminase.

It was somewhat surprising to isolate mutants with two distinct genetic alterations. Mpa^r cannot be a mixture of two populations: it can have no more than 10% wild type Hyp transport and no more than 2% wild type Ade deaminase activity. It is also unlikely that both Hyp transport and Ade deaminase activities are on the same polypeptide. The two genes may be on adjacent DNA so that a single deletion can destroy both. Since the mutant was selected by stepwise increases in drug concentration over 7 weeks, two separate mutations are possible. Both mutations are probably necessary to achieve the 50-fold resistance to MPA. Less MPA-resistant strains may have only one of the mutations. Fortunately, the less MPA-resistant *T. foetus* populations are preserved. It will be interesting to examine Hyp transport and Ade deaminase activity in these strains to determine how the double mutant arose.

* Formycin B inhibition of Ade incorporation into Ade nucleotides could also result from the inhibition of adenosine phosphorylase by the metabolite formycin A [26, 27]. However, similar inhibition of Ade incorporation into Ade nucleotides was observed with hadacidin. The observation that two different adenylosuccinate synthase inhibitors inhibited Ade incorporation into Ade nucleotides suggests that the adenosine phosphorylase–adenosine kinase pathway does not contribute substantially to Ade incorporation into nucleotides.

The mechanism by which Hyp inhibits Xan incorporation into nucleotides is unknown. One possibility is that Hyp may simply outcompete Xan for HGXPRT. Xan was a poorer substrate than Hyp and Gua, as shown in Table 2. A simple calculation based on the fraction inhibited for a substrate and its competitive inhibitor [28] predicts that Xan phosphoribosylation should be 92% inhibited by Hyp in wild type versus 54% inhibited for mpa^r when the cells are growing on TYM: $i = [Hyp]/\{[Hyp] + K_i(1 + [Xan]/K_m)\}$, where $[Xan] = 200\ \mu M$, $K_m = 70\ \mu M$, $K_i = 5\ \mu M$, $[Hyp] = 200\ \mu M$ for wild type and $40\ \mu M$ for mpa^r (from panels A and B of Fig. 6 and Table 2). This predicts that mpa^r can incorporate Xan from TYM medium into the nucleotide pool four times more efficiently than wild type simply by relieving Hyp inhibition of XPRT. We are isolating HGXPRT to test this hypothesis. Alternatively, Hyp inhibition may result from the buildup of some other intermediate, for example IMP, causing product inhibition or some other more complicated mode of regulation.

In summary, we discovered a complex new mechanism of MPA resistance in the protozoan parasite *T. foetus*. Mpa^r rearranged its purine salvage pathway to bypass IMP dehydrogenase, the MPA-sensitive step, by decreasing Hyp transport and Ade deaminase activity. The combination of these two mutations lowered the intracellular concentration of Hyp. In the absence of intracellular Hyp, the parasite will salvage Xan readily from a mixture of purines. Xan incorporation into nucleotides via XMP provided an IMPDH independent route to Gua nucleotides and the parasite was thus MPA resistant.

Acknowledgements—The authors would like to thank Dr Richard L. Miller for helpful discussions and John Barnard for technical assistance. This work was supported by NIH Postdoctoral Fellowship 1F32-GM10504 (L.H.) and NIH Grant AI 19391 (C.C.W.).

REFERENCES

1. Honigberg BM, Trichomonads of veterinary importance. In: *Parasitic Protozoa* (Ed. Kreier JP, Vol. 2, pp. 163–273. Academic Press, New York, 1978.
2. Wang CC, Current problems in anti-parasitic chemotherapy. *Trends Biochem Sci* 7: 354–356, 1982.
3. Wang CC, Verham R, Rice A and Tzeng S, Purine salvage in *Tritrichomonas foetus*. *Mol Biochem Parasitol* **8**: 325–337, 1983.
4. Verham R, Purine and pyrimidine metabolism in *Tritrichomonas foetus*. Ph.D. Dissertation, Department of Pharmaceutical Chemistry, University of California, San Francisco, 1985.
5. Franklin TJ and Cook JM, The inhibition of nucleic acid synthesis by mycophenolic acid. *Biochem J* **113**: 515–524, 1969.
6. Verham R, Meek TD, Hedstrom L and Wang CC, Purification, characterization and kinetic analysis of inosine 5′-monophosphate of *Tritrichomonas foetus*. *Mol Biochem Parasitol* **24**: 1–12, 1987.
7. Wang CC, Verham R, Cheung H-W, Rice A and Wang AL, Differential effects of inhibitors of purine metabolism of two trichomonad species. *Biochem Pharmacol* **33**: 1323–1329, 1984.
8. Diamond LS, The establishment of various trichomonads of animals and man in axenic cultures. *J Parasitol* **43**: 488–490, 1957.
9. Rose LM and Brockman RW, Analysis by high pressure liquid chromatography of 9-β-D-arabinofuranosyladenine 5′-triphosphate levels in murine leukemia cells. *J Chromatogr* **133**: 335–343, 1977.
10. Schweinsberg PD and Loo TL, Simultaneous analysis of ATP, ADP, AMP and other purines in human erythrocytes by high performance liquid chromatography. *J Chromatogr* **181**: 103–107, 1980.
11. Wohlhueter RM, Marz R, Graff JC and Plagemann PGW, A rapid-mixing technique to measure transport in suspended animal cells: applications to nucleoside transport in Novikoff rat hepatoma cells. *Methods Cell Biology* **20**: 211–236, 1978.
12. Bradford MM, A rapid and sensitive method for the quantitation of microgram quantities of protein utilizing the principle of protein-dye binding. *Anal Biochem* **72**: 248–254, 1976.
13. Brox L and Hampton A, Inosine 5′-phosphate dehydrogenase. Kinetic mechanism and evidence for selective reaction of the 6-chloro analog of inosine 5′-phosphate at the inosine 5′-phosphate site. *Biochemistry* **7**: 2589–2596, 1968.
14. Lee H-J, Pawlak K, Nguyen BT, Robbins RK and Sadee W, Biochemical differences among four inosinate dehydrogenase inhibitors, mycophenolic acid, ribavirin, tiazofurin and selenazofurin, studied in mouse lymphoma cell culture. *Cancer Res* **45**: 5512–5520, 1985.
15. Shigeura H and Gordon CN, The mechanism of action of hadacidin. *J Biol Chem* **237**: 1937–1940, 1962.
16. Carson DA and Chang K-P, Phosphorylation and antileishmanial activity of formycin B. *Biochem Biophys Res Commun* **100**: 1377–1383, 1981.
17. Hedstrom L and Wang CC, Purine base transport in wild type and mycophenolic acid resistant *Tritrichomonas foetus*. *Mol Biochem Parasitol* **35**: 219–228, 1989.
18. Smith RA and Kirkpatrick W, The pharmacology of ribavirin. In: *Developments in Antiviral Therapy* (Eds. Collier LH and Oxford T), pp. 133–156. Academic Press, London, 1980.
19. Sweeney MJ, Gerzon K, Harris PN, Holmes RE, Poore, GA & Williams RH, Experimental antitumor activity and preclinical toxicology of mycophenolic acid. *Cancer Res* **32**: 1795–1802, 1972.
20. Huberman E, McKeown CK and Friedman J, Mutagen-induced resistance to mycophenolic acid in hamster cells can be associated with increased inosine 5′-phosphate dehydrogenase activity. *Proc Natl Acad Sci USA* **78**: 3151–3154, 1981.
21. Ullman B, Characterization of mutant murine lymphoma cells with altered inosinate dehydrogenase activities. *J Biol Chem* **258**: 523–528, 1983.
22. Sweeney MJ, Hoffman DH and Esterman MA, Metabolism and biochemistry of mycophenolic acid. *Cancer Res* **32**: 1803–1809, 1972.
23. Mulligan RC and Berg P, Selection for animal cells that express the *Escherichia coli* gene coding for xanthine–guanine phosphoribosyltransferase. *Proc Natl Acad Sci USA* **78**: 2072–2076, 1981.
24. Plagemann PGW and Wohlheuter RM, Permeation of nucleosides, nucleic acid bases and nucleotides in animal cells. *Curr Top Membr Trans* **14**: 225–330, 1980.
25. Hansen BD, Sleeman HK and Pappas PW, Purine base and nucleoside uptake in *Plasmodium berghei* and host erythrocytes. *J Parasitol* **66**: 205–212, 1980.
26. DeWolf WE, Fullin FA and Schramm VL, The catalytic site of AMP nucleosidase. *J Biol Chem* **254**: 10868–10875, 1979.
27. Sheen MR, Kim BY and Parks RE, Purine nucleoside phosphorylase from human erythrocytes. III. Inhibition by the inosine analog formycin B of the isolated enzyme and of the nucleoside metabolism in intact erythrocytes and Sarcoma 180 cells. *Mol Pharmacol* **4**: 293–299, 1968.
28. Segel IH, *Enzyme Kinetics*, pp. 100–107. John Wiley, New York, 1975.